

Characterization of Silica Supported NiMoO₄ Doped with Ce, Cr and Zr Using Thermodesorption Techniques

Rodica Zăvoianu^{*}, Octavian Dumitru Pavel, Anca Cruceanu, Cristina Preda, Crenguța Ștefania Nițu, Emilian Angelescu

University of Bucharest, Faculty of Chemistry, Department of Chemical Technology and Catalysis

Abstract

The acid-base properties of pure NiMoO₄, silica supported NiMoO₄ and silica supported NiMoO₄ doped with Ce, Cr and Zr were investigated using temperature-programmed desorption (TPD) of NH₃ and respectively CO₂. It was found that the presence of dopants modifies the distribution and the strength of acid-base sites. Doping with Ce or Cr leads to the enhancement of the base character of the silica-supported NiMoO₄ and this fact was associated to the increase of the amount of β-NiMoO₄ in these catalysts, which was confirmed by XRD analysis.

Key words: silica supported NiMoO₄, TPD-CO₂, TPD-NH₃, acid-base properties, β-NiMoO₄ stabilisation, doped NiMoO₄

1. Introduction

Nickel molybdates are known to be useful catalysts in the oxidative dehydrogenation and selective oxidation of hydrocarbons [1-6]. The selectivity of these catalysts towards oxidative dehydrogenation is assumed to be strongly influenced by their reducibility and also by the basicity of the surface [7]. Until now, the majority of the studies concerning the physico-chemical properties of the nickel molybdates catalysts were focused on their crystallographic structure, reducibility and electrical conductivity. Some authors showed that better catalytic properties were related to the presence of the β-phase of NiMoO₄ in the catalysts [1,2]. Usually this phase, characterized by the tetrahedral coordination of Mo, is stable only at temperatures higher than 650°C, while below this temperature the α-phase with Mo in octahedral coordination is stable [8-10]. Several studies showed that β-NiMoO₄ might be stabilised at lower temperature either by an excess of NiO [9], or by supporting the active phase on alumina [11-13], or active carbon [14] carriers. Lately, some works of Mazzochia [15,16] claimed that the stabilisation of the β-phase takes place also by supporting the nickel molybdate on silica using sol-gel method. Also,

^{*} Corresponding author: Univ. Bucharest, Fac. Chemistry, Dept. Chemical Technology and Catalysis, Bd. Regina Elisabeta, No.4-12, Sector 3, Bucharest-030018, Romania, Fax: 00-40-21-3159249; e-mail: rzavoianu@chem.unibuc.ro

recently another method, which did not involve sol-gel preparation allowed the synthesis of catalysts containing stoichiometric NiMoO_4 supported on SiO_2 with high amounts of $\beta\text{-NiMoO}_4$, as it was proved by the XRD, FTIR spectroscopy and TG/DTA analyses [17, 18]. The further study of the acid base properties of these catalysts by means of temperature programmed desorption (TPD) of NH_3 , and respectively CO_2 , showed that an increase of the content of $\beta\text{-NiMoO}_4$ is associated to an increase of the basicity [19].

TPD is a rather simple technique for the characterization of catalysts that was first described by Amenomiya and Cvetanovic in 1963 [20, 21]. In TPD studies a sample material previously equilibrated with an adsorbate under well-defined conditions is submitted to a programmed temperature increase. This increase of the thermal energy overcomes the adsorption energies of the previously adsorbed species in the order of their increasing adsorption energy and determines their desorption from the surface. The desorbed molecules are swept by a carrier gas to a detector where they are quantified [22, 23]. Even if the TPD method cannot identify the difference between Brönsted and Lewis sites it can give some indications about the different strength of the sites and about the number of adsorption sites which are still active at the reaction temperature. If the TPD experiments on the same sample are performed with different heating rates, an evaluation of the energy of desorption might be possible.

Up to now, Stern and Grasselli [24] investigated the structure of some cobalt-nickel molybdate catalysts supported on silica doped with P, Bi, Fe, Ce, Cr or V and their activity for the oxidative dehydrogenation of propane. However, the acid-base properties of these doped catalysts were not studied, even if the number and the strength of these sites could influence the adsorption of both reactants and reaction products. Thus, a higher number of basic sites will facilitate the desorption of alkenes (the main reaction product in oxidative dehydrogenation), while a higher number of Lewis acid sites will favour their adsorption and subsequent transformation to secondary reaction products. Since the oxidative dehydrogenation of alkanes takes place at temperatures higher than 350°C , a special attention should be directed towards the determination of the amount of strong base and respectively acid sites, which are still active at these temperatures. Therefore, in the present paper, it was considered to be interesting to study the influence of the dopants on the surface properties of silica supported NiMoO_4 catalysts by means of NH_3 - and respectively CO_2 -TPD. The acid-base properties of the supported catalysts are compared with those of the unsupported stoichiometric NiMoO_4 and correlated to the results of XRD and FTIR analysis.

2. Experimental

The stoichiometric NiMoO_4 was prepared by coprecipitation, at 80°C , using aqueous solutions of $\text{Ni}(\text{NO}_3)_2 \cdot 6\text{H}_2\text{O}$ (Merck, p.a.) (1.2 M) and $(\text{NH}_4)_6\text{Mo}_7\text{O}_{24} \cdot 4\text{H}_2\text{O}$ (Merck, p.a.) (0.04 M). NH_3 aqueous solution 25 w/w % (Merck, p.a.) was added to the molybdate's solution to ensure the transformation of the ammonium heptamolybdate into ammonium molybdate, $(\text{NH}_4)_2\text{MoO}_4$, which reacts in equimolar

amounts with the nickel nitrate. The respective quantity of NH₃ solution allowed adjusting the pH of the reaction mixture to 5.2.

The silica support was obtained by precipitation, at 80°C, using aqueous solutions of Na₂SiO₃ (Fluka p.a.) (10 w/w %) and HNO₃ (Merck, p.a.) (1 N). The gel obtained at basic pH (pH = 10) was washed with distilled water until the neutral pH of the washing water was reached and it was further utilised in the preparation of silica supported catalysts. The drying of this gel during 12 hours at 110°C followed by calcination at 550°C under dry air flow (0.5 cm³s⁻¹) during 4 hours yielded silica with a specific surface area of 450 m².g⁻¹.

The silica supported nickel molybdate catalyst (NiMoSi) was obtained by precipitating NiMoO₄ over the support at 80°C, using a method similar to that previously described for the preparation of the pure NiMoO₄. The appropriate amounts of nickel nitrate, ammonium heptamolybdate, and respectively NH₃ solutions were added simultaneously, under stirring, to an aqueous suspension of the support. The concentration of NiMoO₄ in the supported catalyst was 0.2 moles/100 grams (e.g. 40 w/w %).

Doped catalysts NiMoD_{1%}Si, with an atomic ratio Ni:Mo:D = 1:1:0.01 (D= Ce, Cr, or Zr), were prepared in a manner similar to that used for the preparation of silica supported NiMoO₄, by adding the adequate amount of an aqueous solution containing the dopant. The concentration of the dopant expressed as amount of oxide in the final catalysts was 0.1 w/w% Cr₂O₃; 0.2 w/w% ZrO₂ and respectively 0.3% CeO₂. Ce(NO₃)₄•4H₂O, Cr(NO₃)₃•6H₂O and ZrO(NO₂)₂ (Merck p.a.) were used as dopant agent sources.

After the precipitation of the active phase, the excess water was slowly evaporated at 85°C. Then, the precursors obtained were dried overnight at 110°C and calcined, under dry airflow (0.5 cm³s⁻¹), at 550°C for 4 hours.

The chemical composition of the catalysts was determined using elemental analysis. Catalysts were also characterized by XRD, FTIR spectroscopy, and BET analysis using liquid nitrogen for determining the surface area and pore volume. The XRD analyses of the catalysts were recorded at room temperature with a Philips diffractometer using Cu K α radiation and a Ni filter. The diffraction pattern of the unsupported NiMoO₄ showed the characteristic diffraction lines of the pure α phase at 2 θ =14.5, 24.3, 26.1, 29, 32.8, 38.7, 41.3, 43.9 and 47.6° according to JCPDS and ASTM files [25,26], the most intense line being the one at 2 θ = 29°. The FTIR spectra of the catalysts in the range 450 - 4050 cm⁻¹, (64 scans/min, 4 cm⁻¹ resolution) and were recorded with a Beckmann spectrophotometer, using KBr pellets technique.

TPD experiments were performed at atmospheric pressure using an experimental set-up consisting of a quartz micro-reactor connected on-line to a TCD. A gaseous mixture containing 5 mol.% NH₃ in argon was used for TPD-NH₃, while in the case of TPD-CO₂ the gaseous mixture contained 5 mol.% CO₂ in nitrogen. All the gases used were of high purity (99.995%) and their feeds were controlled with flow controllers. Prior to adsorption, each sample (*ca.* 300 mg) was kept under argon

flow, at 550°C, until the complete removal of the adsorbed impurities. The sample was cooled down to 25°C and pulses of the adsorbing gas introduced until the saturation of the surface. The physisorbed gas was removed by passing argon for 30 minutes. The thermodesorption was then performed by heating the sample up to 500°C in TPD-NH₃ experiments and respectively 700°C for TPD-CO₂, at 10°C/min, under inert gas flow (1 mL/s) while the signal of the detector is recorded generating the characteristic TPD plot.

The acidities and basicities were quantified by integration of the desorption curves of TPD-NH₃ and TPD-CO₂, respectively. The areas under the curves are considered as proportional to the number of moles of gas desorbed from the surface. The number of moles of NH₃ and CO₂ desorbed per gram of catalyst are hereafter referred to as A_s and B_s . The temperatures corresponding to the maximums appearing on the curves are designated as $T_{\max,i}$. Also, the TPD plots of the catalysts were deconvoluted using the ORIGIN-5 computer program for fitting multi-peaks Gauss function. It has been assumed that the area under each deconvolution curve is proportional to the number of a certain type of acid/base sites. Since the total area under the TPD-plot is the sum of the areas situated under each deconvolution curve, by dividing the area under each curve to the total area, the fraction of acid/base sites of different strength from the total amount could be estimated. The number of sites corresponding to each category can be estimated by evaluating its percentage from the total amount of sites (A_s , and respectively B_s).

3. Results and discussion

The thermograms obtained for the temperature programmed desorption of NH₃ and respectively CO₂ are presented in fig. 1. The specific surface areas of the catalysts determined by BET method and the results obtained by the integration of the TPD-plots and the corresponding deconvolution curves along with the distribution of the acid/base sites are summarised in Table 1.

As it may be seen from fig. 1 and the data presented in Table 1, the temperatures characteristic for the maximum intensity of NH₃ and respectively CO₂ desorption deconvoluted curves are different for each catalyst.

These differences are related to the different strength for each type of acid and respectively base sites. In what concerns the acid sites, it is generally considered that $T_{\max1}$ lower than 200°C can be ascribed to weak acid sites, $T_{\max2}$ in the range 200-350°C is characteristic for medium strength acid sites, while $T_{\max3}$ higher than 350°C is related to strong acid sites [22].

Based on similar considerations, Choudhary [23] proposed the following classification for the base sites: very weak base sites ($T_{\max1}$ in the range 50-150°C), weak base sites ($T_{\max2}$ in the range 150-300°C), medium strength base sites ($T_{\max3}$ in the range 300-450°C), strong base sites ($T_{\max4}$ from 450 up to 650°C).

Since most of the processes using as catalysts nickel molybdates or supported nickel molybdates are taking place at high temperatures, a special attention should be focused on the strong acid and base sites which are still active for the adsorption-desorption of the reactants and reaction products under the operating conditions. The

experimental data showed that the strength of the strong acid sites as a function of the value of T_{max} increases as it follows:



while, in the case of the strong base sites the order of their increasing strength is:

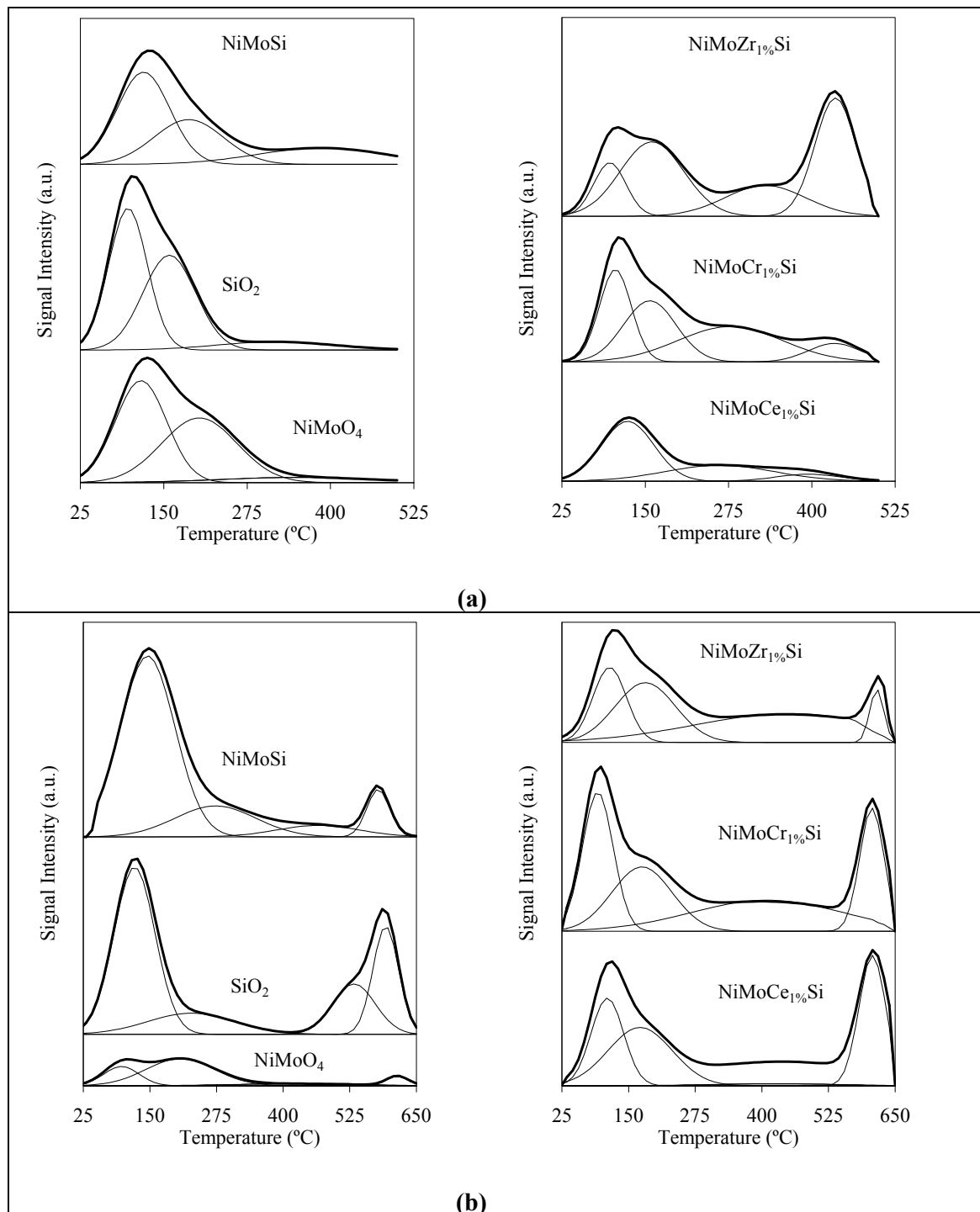


Fig. 1. Thermograms obtained by TPD-NH₃ (a) and TPD-CO₂ (b) for the unsupported NiMoO₄, the SiO₂ support, and the silica supported NiMoO₄ catalysts

Several aspects should be highlighted. Thus, Zr-doping leads to the apparition of the strongest adsorption sites both acid and base, while the concentration of strong acid sites is much higher than the concentration of strong base sites. Ce-doped catalyst has the higher concentration of strong base sites and the lowest concentration of strong acid sites. The deconvolution of the thermograms for the undoped NiMoO₄ catalysts and the Ce-doped catalyst evidenced three types of acid sites. Probably due to the basic character of Ce, this dopant does not generate a new type of acid sites. On the contrary, the doping with Cr and Zr, which have more acid character than Ce, lead to the apparition of a fourth type of acid sites. This thing may be a consequence of generating new acid sites specific either to the interaction between the doping agent and the support [27], or to the formation of mixed phases such as ZrMo₂O₈ H₂ZrSi₂O₈ [28, 29].

Table 1. Specific surface areas of the catalysts and the results of TPD experiments

Catalyst	S _{sp} BET (m ² /g)	TPD-NH ₃			TPD-CO ₂		
		Total acidity* (A _s)	T _{max,i} (°C)	Distribution (%)	Total basicity** (B _s)	T _{max,i} (°C)	Distribution (%)
SiO ₂	450	65.2	T _{max,1} =96	43.7	72.3	T _{max,1} =121	50.4
			T _{max,2} =158	8.4		T _{max,2} =227	13.5
			T _{max,3} =318	47.9		T _{max,3} =533	15.7
						T _{max,4} =592	20.3
NiMoO ₄	33.2	59.1	T _{max,1} =116	47.9	39.9	T _{max,1} =96	22.8
			T _{max,2} =203	44.7		T _{max,2} =207	61.6
			T _{max,3} =351	7.4		T _{max,3} =424	8.9
						T _{max,4} =614	6.8
NiMoSi	220	44	T _{max,1} =120	48.2	56.9	T _{max,1} =146	68.7
			T _{max,2} =187	30.7		T _{max,2} =273	7.3
			T _{max,3} =387	21.1		T _{max,3} =466	6.5
						T _{max,4} =578	7.5
NiMoCe _{1%} Si	205	30.8	T _{max,1} =124	59.4	65.2	T _{max,1} =110	21.2
			T _{max,2} =262	32.5		T _{max,2} =172	28
			T _{max,3} =395	8.4		T _{max,3} =434	24.6
						T _{max,4} =607	26.2
NiMoCr _{1%} Si	239	38.7	T _{max,1} =90	27.2	60.4	T _{max,1} =92	27.1
			T _{max,2} =143	29.8		T _{max,2} =175	24.4
			T _{max,3} =268	34.1		T _{max,3} =410	29.6
			T _{max,4} =431	8.9		T _{max,4} =607	18.9
NiMoZr _{1%} Si	228	50.6	T _{max,1} =97	12.5	46.9	T _{max,1} =115	20.5
			T _{max,2} =160	34.3		T _{max,2} =181	29.3
			T _{max,3} =330	17.9		T _{max,3} =442	44.3
			T _{max,4} =435	35.3		T _{max,4} =616	5.9

*- total acidity = (A_s) = total number of acid sites expressed as μmoles NH₃/g

**-total basicity = (B_s) = total number of base sites expressed as μmoles CO₂/g

By comparing the number of acid sites (A_s) and base sites (B_s), the above presented results show that silica support prepared by precipitation at pH=10 has a slightly base character (B_s/A_s =1.1), while the pure NiMoO₄ presents a slightly acid character (B_s/A_s =0.7). On silica support, the amount of strong acid sites (T_{max3}=318°C) exceeds the amount of weak ones, while in the case of NiMoO₄ weak acid sites are prevailing. Also, the weak base sites (T_{max1}=121°C) prevail on the strong ones in the case of silica support, while the pure NiMoO₄ has the highest concentration of medium

strength base sites ($T_{\max 2}=207^{\circ}\text{C}$). Supporting the nickel molybdate on silica carrier leads to an increase of the base character of the catalyst, since the ratio $B_s/A_s = 1.3$. The same effect is obtained in the case of Ce ($B_s/A_s = 2.1$) and Cr-doped catalysts ($B_s/A_s = 1.6$). On the contrary, in the case of Zr-doped catalyst the acid character is prevailing, $B_s/A_s = 0.9$. However, the Zr-doped catalyst may be considered more basic than the unsupported nickel molybdate, since its B_s/A_s ratio is higher than 0.7 (e.g. value corresponding to pure NiMoO₄). Therefore, it may be concluded that all silica-supported catalysts are more basic than the unsupported NiMoO₄. This fact could be considered as indicating the stabilisation of the β -phase of NiMoO₄ by its deposition on silica, since it has already been shown that an increase of the content of β -NiMoO₄ leads to a decrease of the acidity [19], due to the fact that in the structure of this phase the Ni sites which are responsible for the base character are more exposed, as it can be seen in fig. 2.

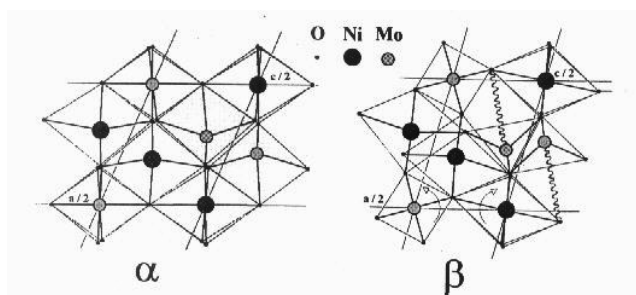
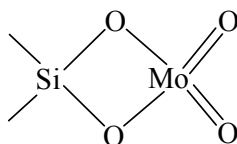


Fig. 2. Structures of α - and β -NiMoO₄ presented by Del Rosso et al. [30]

Indeed, this assumption was confirmed by the results of the XRD-analysis of the silica-supported catalysts presented in fig. 3. Thus, in the XRD patterns of all silica supported NiMoO₄ catalysts, besides the diffraction lines characteristic to the α phase, some of the lines characteristic to the β phase at $2\theta = 14.4, 25.4, 26.7, 27.3, 28.8, 32.7, 33.9, 43.8$ and 47.5° , the most intense being the one at 26.7° [10,15] are also present, indicating that supporting the nickel molybdate by its precipitation directly on silica support allows the stabilisation of the β phase even at room temperature. By evaluating the relative intensity of the diffraction lines it may be noticed that in all supported catalysts the β -NiMoO₄ is the prevailing phase. This fact may be a consequence of the formation of tetrahedral Mo sites such as (I) following the interaction between acid species containing molybdenum and the basic sites of silicagel [31].



(I)

In the diffraction patterns of the doped catalysts the lines corresponding to the dopant oxides could not be evidenced probably due to their low concentration (less than 0.5%). However, there are some differences between the diffraction patterns of the doped catalysts that may be pointed out. Thus, it may be seen that doping the

catalyst with Ce, enhances mainly the stabilisation of the β -phase, the doping with Cr leads to higher amounts of both α - and β -phases probably because Cr species can adopt both octahedral and tetrahedral configuration, while Zr doping decreases the crystallinity of the NiMoO_4 since the XRD pattern presented a higher level of background signal.

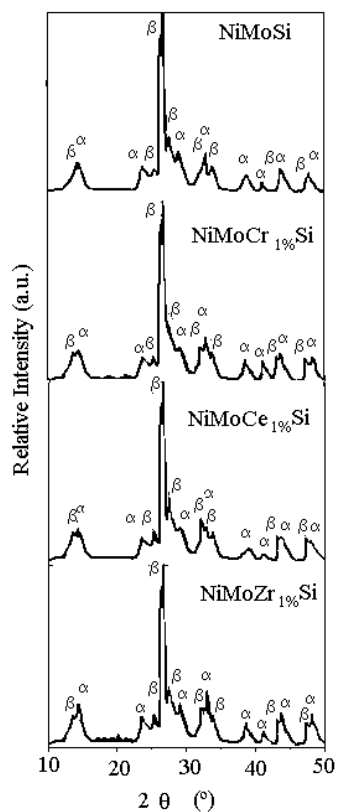


Fig. 3. XRD patterns

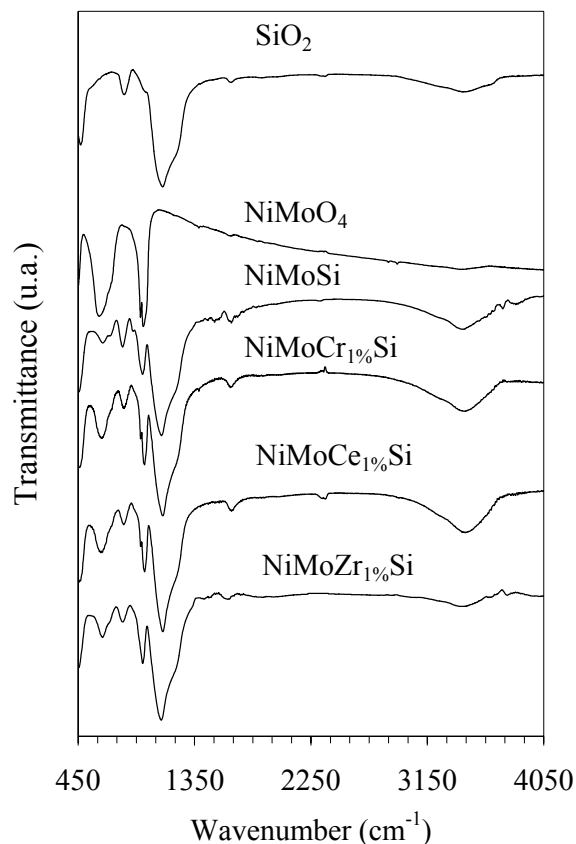


Fig. 4. FTIR spectra

Another indication of the more basic character of silica supported nickel molybdate catalysts is given by the FTIR spectra presented in fig. 4. The most significant differences between spectra are noticed in the region $3200\text{--}3600\text{ cm}^{-1}$ where the vibrations in hydroxyl groups appear. Thus, the intensities of these bands increase in the same order as the base character. Besides that, all the spectra of supported catalysts present the most intense bands of the support at $470, 800, 1100\text{ cm}^{-1}$, and the bands at $610, 935, 958\text{ cm}^{-1}$, characteristic to NiMoO_4 [1-3]. The band corresponding to the tetrahedral coordination of Mo in $\beta\text{-NiMoO}_4$ at 880 cm^{-1} is overlapped by the band at 800 cm^{-1} corresponding to the support and none of the characteristic lines for the doping agents were noticed, due to their low concentration.

4. Conclusions

The above-presented results showed that doping silica-supported NiMoO_4 by Ce, Cr and Zr lead to a better stabilisation of the β -phase of NiMoO_4 and to modification

of the distribution and strength of the acid and base sites. The increase of the amount of β -phase in the doped catalysts is accompanied by an increase of their relative basicity as it was revealed by TPD analyses. The modifications of the basicity may be correlated with the acid-base properties of the doping oxide. Thus, due to its basic character, Ce is the dopant that enhances the most the basicity of the catalyst, while dopants with more intense acid character such as Cr –and Zr- lead to the apparition of new types of acid sites.

Acknowledgements

The financial support of this work by of CNCSIS through CERES programme, grant 3-106, is gratefully acknowledged.

References

- Mazzocchia, C., Aboumrar, C., Diagne, C., Tempesti, E., Herrmann, J.M., Thomas, G., *Catal. Lett.*, **10**, 181 (1991).
- Maldonado-Hodar, F.J., Madeira, L.M., Portela, M.F., *J. Catal.*, **164**, 399 (1996).
- Mazzocchia, C., Del Rosso, R., Centola, P., *An. Quimica*, **79**, 108, (1980).
- Kaddouri, A., Mazzocchia, C., Tempesti, E., *Appl. Catal. A: General*, **169**, L3, (1998).
- Maldonado-Hodar, F.J., Madeira, L.M., Portela, M.F., Martin Aranda, R.M., Freire, F., *J. Molec. Catal. A-Chem.*, **111**, 313, (1996).
- Madeira, L.M., Maldonado-Hodar, F.J., Portela, M.F., Freire, F., Martin Aranda, R.M., *Appl. Catal. A: General*, **135**, 137, (1996).
- Madeira, L.M., Portela, M.F., *Catalysis Reviews*, **44(1)**, 1-40 (2002)
- Smith, G.W., *Acta Crystallogr.* **15**, 1954 (1962)
- Plyasova, L.M., Ivanchenko, I.Yu., Andrushkevich, M.M., Buyanov, R.A., Itenberg, I.Sh., Khranova, G.A., Karachiev, L.G., Kustova, G.N., Stepanov, G.A., Tsailingol'd, A.L., Philipenko, F.S., *Kinet. Katal.*, **14(4)**, 1010 (1973).
- Di Renzo, F., Mazzocchia, C., *Therm. Acta*, **85**, 139 (1985).
- J.L. Brito and J. Laine, *J. Catal.*, **139**, 540 (1993).
- H. Topsøe, B.S. Clausen, N. Topsøe and E. Padersen, *Ind. Eng. Chem. Fund.*, **25**, 25 (1986).
- G. Gualda and S. Kasztelan, *J. Catal.*, **161**, 319 (1996).
- Calafat, A., Laine, J., López-Agudo, A., Palacios, J.M., *J. Catal.*, **162**, 20 (1996).
- Cauzzi, D., Deltratti, M., Predieri, G., Tiripicchio, A., Kaddouri, A., Mazzocchia, C., Tempesti, E., Armigliato, A., Vignali, C., *Appl. Catal. A:General*, **183**, 125-135 (1999).
- Kaddouri, A., Tempesti, E., Mazzocchia, C., *Mat. Res. Bull.*, **39**, 695-706, (2004)
- Zăvoianu, R., Dias, C. R., Portela, M. F., in *Heterogeneous Catalysis*, L. Petrov, Ch. Bonev, G. Kadinov (Eds.), 2000 Institute of Catalysis, Bulgarian Academy of Sciences, Sofia, p. 411-416
- Dias, C. R., Zăvoianu, R. Portela, M.F., *Catalysis Communications*, **3**, 85-90, (2002)
- Zăvoianu, R., Dias, C.R., Portela, M.F, *React. Kinet. Catal. Lett.*, **72**, 201, (2001)
- Amenomiya, Y., Cvetanovic, R.J., *J. Phys. Chem.*, **67**, 144 (1963)
- Cvetanovic, R.J., Amenomiya, Y., *Catal. Rev*, 21 (1972).
- Webb, P.A., Orr, C., in “*Analytical Methods in Fine Particle Technology*”, Micromeritics Instrument Corporation, Norcross, GA USA 1997, ISBN 0-9566783-0-X, Chapter 6, p. 219, 235-239; 251-252 TPDNH3
- Choudhary, V.R., Rane, V.H, *Catal. Lett.*, **4**, 101-106, (1990) TPD-CO2
- Stern, D.L., Grasselli, R.K., *J. Catal.*, **167**, 550-559 (1997)
- JCPDS Powder Diffraction File, International Center for Diffraction data, Swarthmore, PA, 1989

26. ASTM files: 33-948 (NiMoO₄); 13-128 (NiMoO₄·xH₂O); 5-0452 (MoO₂ monoclinic); 33-069 (MoO₃ orth.); 21-569 (MoO₃ hex.); 4-0835 (NiO, cubic); 14-117 (Ni(OH)₂ hex.)
27. Fajdala, K.L., Don Tilley, T., *J. Catal.*, **218**, 123-134 (2003)
28. Liu, Z., Chen, Y., *J. Catal.*, **177**, 314-324 (1998)
29. Popescu, A., Angelescu, E., in “*Procese Catalitice în Chimia Hidrocarburilor*”, Ed. Didactică și Pedagogică București, 1976, p. 32
30. Del Rosso, R., Kaddouri, A., Mazzochia, C., Gronchi, P., Centola, P., *Catal. Lett.* **69**, 71-78 (2000)
31. Suzuki, T., Hirai, T., Tanaka, T., *J. Mol. Catal.*, **49**, L43, (1989)